# Initiation and runout characteristics of debris flow surges in Ohya landslide scar, Japan

# Initiation and runout characteristics of debris flow surges in Ohya landslide scar, Japan

Fumitoshi Imaizumi[a], Takeshi Masui[b], Yushi Yokota[c], Haruka Tsunetaka[d], Yuichi Hayakawa[e], Norifumi Hotta[f]

a Faculty of Agriculture, Shizuoka University
836 Ohya, Shizuoka, 422-8529, Japan

b Bureau of Industrial and Labor Affairs, Tokyo Metropolitan Government
Shinjuku-ku, Tokyo, 163-8001, Japan

c Graduate school of Integrated Science and Technology, Shizuoka University
836 Ohya, Shizuoka, 422-8529, Japan

d Forest Research and Management Organization
1 Matsunosato, Tsukuba, 305-8687, Japan

e Faculty of Environmental Earth Science, Hokkaido University
N10W5, Sapporo, 060-0810, Japan

f Faculty of Agriculture, The University of Tokyo
1-1-1, Yayoi, Bunkyo-ku, Tokyo, 113-8657, Japan

Correspondence to: Fumitoshi Imaizumi (imaizumi@shizuoka.ac.jp)

## Abstract

The characteristics of debris flows (e.g., velocity, discharge, kinematic energy) are highly dependent on surges incurring abrupt changes to flow height, velocity, and boulder concentration. Therefore, understanding the initiation and runout characteristics of surges is essential when planning debris flow mitigation. Monitoring performed using 10 time-lapse cameras (TLCs) in Ohya landslide, central Japan, where debris flows occur frequently due to mobilization of storage (i.e., talus cone and channel deposits), allowed us to obtain data on a series of surge processes, from initiation to termination, which occurred during each debris flow event. We also analyzed temporal changes in the spatial distribution of storage in the debris flow initiation zone, associated with sediment supply from hillslopes and evacuation of sediment by the occurrence of debris flows, through periodic measurements of topography using unmanned aerial vehicles (UAVs). Debris flow surges were mainly induced by repetitive mass movement of storage through the erosion of channel deposits by overland flow, sliding of channel deposits, and sediment and water supply from channel banks and tributaries. Development of a spontaneous wave on the flow surface was not an important formation process of surges in the Ohya landslide. Many debris flow surges initiated at channel sections with deep storage (>2 m in depth), located less than 30 m below a junction with a tributary, when the maximum 10-minute rainfall intensity exceeded 5 mm. Partly saturated flow, which has an unsaturated layer in its upper part, was the predominant flow type in the steep initiation zone, while fully saturated flow was predominant in the gentle transportation and deposition zones. Flow type often changed as the surges descended. Partly saturated flow was predominant when the volume of storage in the initiation zone was large, whereas fully saturated flow was predominant when the volume of storage was small. When we compared debris flows with similar total sediment volume, travel distance was long when fully saturated flow with high flow mobility was predominant because of the small volume of storage in the initiation zone. The volume of storage also affected flow path avulsion on the debris flow fan by controlling the flow mobility of surges. Consequently, the spatial distribution and total volume of storage are important factors controlling the initiation location, predominant flow type, and termination location of surges.

*Key words*: Debris flow, Surge, Initiation mechanism, UAV, Field monitoring, Sediment storage

## 1. Introduction

Debris flows are one of the most destructive geomorphic processes because of their high velocity, kinematic energy, and large volume of mobilized sediment. Such characteristics are highly dependent on surges incurring abrupt changes in discharge, velocity, and boulder concentration (Coussot and Meunier, 1996; Arattano, 1999; Hürlimann et al., 2003; Berger et al., 2011b; Arattano et al., 2012; Abancó et al., 2014). Therefore, understanding the initiation and runout characteristics of surges is essential when planning debris flow mitigation (Arattano, 1999).

Several initiation mechanisms of debris flows, such as the transition of landslide sediment into a debris flow (Imaizumi et al., 2008; Ogiso and Yomogida, 2015; Iverson and George, 2016), erosion of channel deposits by overland flow (Coe et al., 2008; Gregoretti and Dalla Fontana, 2008; Degetto et al., 2015), and failure of a landslide dam (Chen et al., 2004; Chen et al., 2014), have been reported based on field surveys. Many of these studies estimated debris-flow initiation mechanisms based on field surveys conducted after debris flow events and field monitoring in the transportation and deposition zones of debris flow torrents. However, data on the initiation mechanism of individual surges are limited (Imaizumi et al., 2016b) because of the difficulty of monitoring of debris flows in their initiation zone (Berti et al., 1999; Kean et al., 2013). Imaizumi et al. (2016b) observed a series of mass movements initiating debris flow surges at the Ohya landslide, Japan, where a large amount of sediment is stored as channel deposits and talus slopes. On the other hand, some laboratory analyses of flow mechanisms have concluded that a single-source mass can develop into multiple surges as a result of mechanical instability within a flow (Iverson, 1997; Major, 1997). Nevertheless, a common understanding of the initiation mechanisms of surges has yet to be obtained.

The volume of debris flow material in the initiation zones (e.g., channel deposits and talus slopes) changes over time in association with sediment supply from hillslopes and the evacuation of sediment by debris flows and fluvial processes (Bovis and Jakob, 1999; Imaizumi et al., 2006; Berger et al., 2011a; Theule et al., 2012). Previous studies have pointed out that the rainfall threshold for occurrence of debris flow varies over time, even in a single torrent affected by changes in the volume of debris flow material (Bovis and Jakob, 1999; Jakob et al., 2005; Schlunegger et al., 2009; Chen et al., 2012; Theule et al., 2012). The initiation point of debris flow also varies among events, being affected by the spatial distribution of the storage (Coe et al., 2008; Berger et al., 2011b). Therefore, the accumulation condition of debris flow material is likely an essential factor for explaining the timing and initiation location of debris flows and individual debris flow surges. The accumulation condition of debris flow material can be interpreted easily these days due to the development of measurement methods such as stereophotography using an unmanned aerial vehicle (UAV) (e.g., Schraml et al., 2015; Neugirg et al., 2016).

It is known that flow characteristics (e.g., solid fraction, boulder size, travel distance) differ among debris flow events (Okano et al., 2012; Kean et al., 2013; Hürlimann et al., 2014; De Hass et al., 2018), and even among different surges during a single debris flow event (Berger et al., 2011b; Imaizumi et al., 2017). Rainfall pattern, particle size (mean and range), and the volume of transported material are considered potential factors controlling debris flow type (Okano et al., 2012; Kean et al., 2013; Hürlimann et al., 2014; Takahashi, 2014; Gregoretti et al., 2016). However, how rainfall pattern and the volume of debris flow material affect the flow characteristics of surges remains unclear.

Field monitoring conducted at multiple sites along a debris flow torrent has revealed that flow characteristics of surges change as the surge migrates downstream, being influenced by the channel gradient, and by the erosion and deposition of sediment (Takahashi, 1991, Berger et al., 2011b; Arattano et al., 2012). Therefore, it is possible that the characteristics of surges in transportation and deposition zones of debris flows do not correspond to those in initiation zones. Flume experiments and theoretical studies have revealed that erosion and deposition of sediment are controlled by channel gradient and flow velocity (Takahashi, 1991; Iverson and Ouyang, 2015). Because the flow characteristics of surges change within several to a few tens of seconds (Hürlimann et al., 2003; Arattano et al., 2012), monitoring with a short recording interval at multiple sites is needed to clarify changes in flow characteristics of surges as they flow.

In the Ichinosawa catchment within the Ohya landslide scar, central Japan, intensive field monitoring has been undertaken since 1998 (Imaizumi et al., 2005; Imaizumi et al., 2006). This site is suitable for debris flow monitoring because of the high frequency of debris flows (about three or four events per year) that occur due to the mobilization of storage around channels (i.e., talus cone and channel deposits). Both fully saturated and partly saturated debris flows, where the latter type have an unsaturated layer in their upper part, have been observed frequently in the Ichinosawa because of the steep terrain (Imaizumi et al., 2017). The accumulation condition of the storage varies with time, resulting in the occurrence of various types of debris flows, such as fully and partly saturated debris flows (Imaizumi et al., 2017).

The aim of this study was to clarify the initiation and runout characteristics of debris flow surges based on field monitoring in the Ichinosawa, including periodic measurement of topography using UAVs and intensive monitoring using time-lapse cameras (TLCs). The specific objectives of the study were to (1) clarify the initiation timing, location, and mechanism of surges; (2) clarify the characteristics of runout and termination of surges; and (3) reveal the contribution of each surge to the net change of topography during an entire debris flow.

## 2. Study site

We conducted field monitoring within the Ohya landslide scar in the Southern Japanese Alps (Fig. 1). The Ohya landslide, which was initiated during an earthquake in A.D. 1707, has a total volume of 120 million $m^3$ (Tsuchiya and Imaizumi, 2010). The climate at the site is characterized by high annual precipitation (about 3,400 mm) (Imaizumi et al., 2005). Heavy rainfall (i.e., total rainfall >100 mm) occurs during the rainy season from June to July, and during the autumn typhoon season from August to October. The outcropping bedrock is composed of well-jointed sandstone and highly fractured shale of Paleogene age.

It is south-facing with an altitude ranging between 1270 and 1905 m a.s.l., an area of 0.3 $km^2$, and channel length of ca. 1000 m. The Ichinosawa catchment can be divided into two sections, upper and lower Ichinosawa, separated by a waterfall named "Ohya-ohtaki" located at 1,450 a.s.l. (P20 in Fig. 1b).

The upper Ichinosawa is the initiation zone of debris flows and is characterized by a deeply incised channel and high and steep slopes (40–65°). Seventy percent of the slope is scree and outcropping bedrock; the remaining thirty percent is covered with forest, shrubs, and tussocks. Unconsolidated sediment, ranging from sand particles to boulders (Imaizumi et al., 2016b), is located in the channel bed and talus cones (Imaizumi et al., 2006). Freeze–thaw, which promotes rockfall and dry ravel, is the predominant sediment infilling mechanism (Imaizumi et al., 2006). The storage volume displays seasonal changes caused by sediment supply from hillslopes in winter and early spring, and evacuation of storage due to the occurrence of debris flows in summer and autumn (Imaizumi et al., 2006). Stored sediment has never been completely eroded by debris flows. The channel gradient is mostly steeper than 25° and approaches the slope gradient of talus slope (37.3°; Imaizumi et al., 2017) in the uppermost part of the monitoring section (Fig. 2).

The lower Ichinosawa is a debris flow fan, within which a large proportion of debris flows terminate. Because bedrock has never been exposed in the debris flow fan, the depth of channel deposits is not known in this area. The depth of deposits in the debris flow fan is estimated to be at least 5 m based on previous channel bed changes interpreted visually by periodic field surveys conducted since 1998. The Ichinosawa torrent joins the Hontani torrent at 1300 m a.s.l., becoming the Ohya River. Some debris flows pass through the junction with the Hontani torrent (e.g., one debris flow every several years) and flow down the Ohya River (Imaizumi et al., 2016a). The channel gradient in the lower Ichinosawa is mainly in the range of 15–20° (Fig. 2).

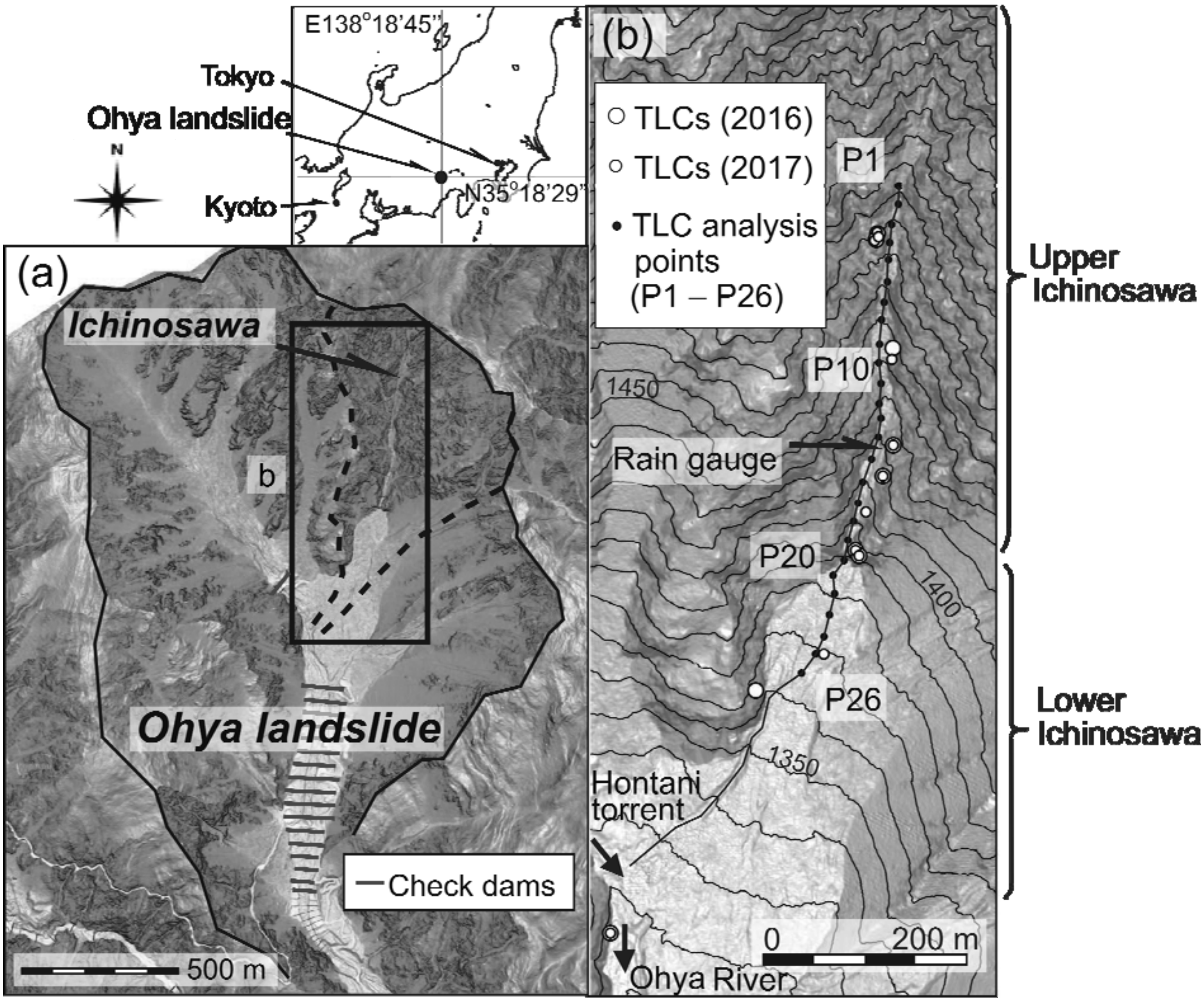


**Figure 1.** Map of the Ohya landslide and Ichinosawa catchment. (a) Entire Ohya landslide, which is surrounded by a black solid line. (b) Monitoring sites in the Ichinosawa catchment. Gentler and steeper terrains are expressed by light and dark colors, respectively. The longitudinal topography along the black line in the torrent is shown in Fig. 2.

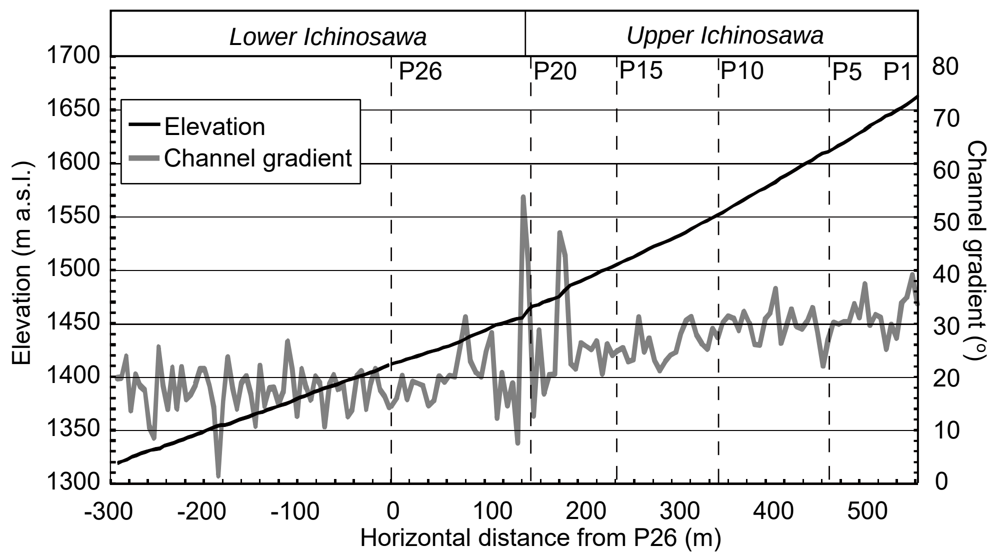

**Figure 2.** Longitudinal profile of the Ichinosawa torrent on August 21, 2016. The channel gradient of each 5 m section is also shown in the figure.

# 3. Methodology

## 3.1. Debris flow monitoring

Eight TLCs (TLC200 Pro; Brinno) were installed along the Ichinosawa torrent with a spacing of about 80 m in the spring of 2016 to capture initiation, runout, and termination processes of debris flow surges. Another camera was installed near the junction with the Hontani torrent. In addition, two more cameras were installed along the Ichinosawa torrent in the spring of 2017, and one previously installed camera was removed. The interval of the TLCs was set at 15 s. We set 26 analysis points (P1 to P26) along the main channel of the Ichinosawa with a spacing of about 20 m to interpret the arrival timing of debris flow surges using TLC images. Some points (P4, P7, P17, P18, and P20 in 2016 and P4, P7, P8, and P18 in 2017) could not be analyzed because they were not covered by TLC images. We visually identified temporal changes of flow type (partly and fully saturated flow) during debris flow events from TLC images based on the existence of interstitial water on the flow surface (Imaizumi et al., 2017). The fully saturated flows are turbulent, and are characterized by a black surface due to high concentrations of silty sediment, sourced from shale in the interstitial water, completely filling the matrix of boulders. In contrast, muddy water is not identified in the flow surface matrix of partly saturated flows. The debris flow surges were classified into three types based on the flow type: surges in which only fully saturated flow was identified (Fig. 3a), surges in which both partly and fully saturated flows were identified (Fig. 3b), and surges in which only partly saturated flow was identified (Fig. 3c). In the Ichinosawa torrent, there are many small mass movements with short travel distances (< 20 m) associated with erosion by surface flow in the channel and failure of channel deposits and talus slopes (Imaizumi et al., 2016b). These mass movements are sometimes separate from the general debris flow, which is a mixture of sediment and water with a long travel distance (Coussot and Meunier, 1996). However, because these mass movements possibly affect the formation of debris flow surges, we interpreted all of these small mass movements as surges.

To monitor rough changes in water height, a semiconductor-type water pressure sensor (S & DLmini; Oyo Co.), which monitored hydrostatic pressures up to 49 kPa with an accuracy of ± 3%, was placed in holes dug in the bedrock of the channel bed around P19. Although we installed the sensor in the channel section, where bedrock is usually exposed, deposition of sediment over the bedrock sometimes occurred. In such cases, the water level was the sum of the flow depth and the thickness of the deposits over the bedrock. Because the water height measured by a water pressure sensor is potentially affected by the density of sediment in interstitial water and the dynamic pressure of the flow, it was not used for detailed analysis.

Precipitation, which is an important trigger of debris flows in the Ohya landslide (Imaizumi et al., 2017), was measured with a logging interval of 1 min using a tipping bucket rain gauge (0.2 mm for one tip) located in an open area near P14 (Fig. 1b).

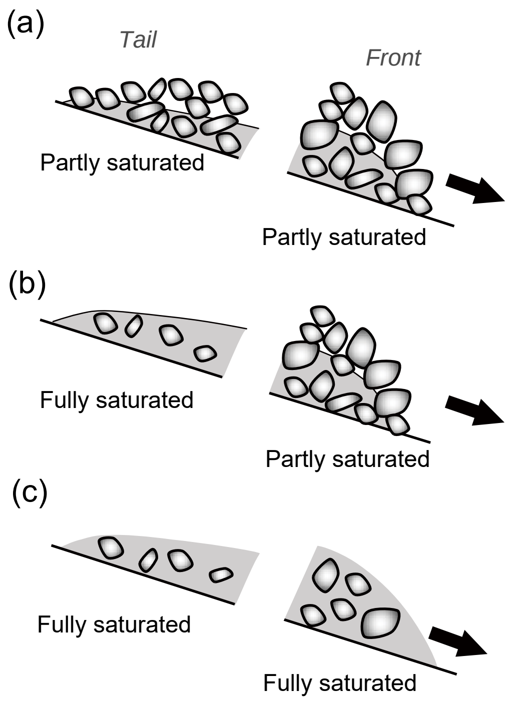


**Figure 3.** Schematic diagram of surge types. (a) Surges in which only partly saturated flow was identified. (b) Surges in which both partly and fully saturated flows were identified. (c) Surges in which only fully saturated flow was identified.

### 3.2. Periodic measurement of channel topography

Temporal changes in the surface topography of storage in the Ichinosawa associated with the occurrence of debris flows were observed by periodic photography from 50 to 100 m above ground level using UAVs

(Phantom 3 and Phantom 4 Pro; DJI). The entire debris flow channel was covered by 700 to 1000 photographs in each period. Point clouds of ground surface topography were constructed from the photographs taken by UAVs using software for structure from motion (SfM) analysis (Photoscan; Agisoft). Coordinate values in a JGD2000 rectangular coordinate system at about 20 ground control points (GCPs), which were used to provide a coordinate system for the point clouds, were positioned according to static measurements obtained using global navigation satellite system (GNSS) devices (TOPCON, GRS-1), and according to real-time kinematic (RTK) measurements obtained using GNSS devices (Hemisphere, A101, A325, and R320). Digital elevation models (DEMs) with a grid size of 0.1 m were also built using Photoscan and a triangulated irregular network (TIN) model (Table 1).

Bedrock topography beneath channel deposits in the upper Ichinosawa was estimated from 1-m grid DEMs obtained by airborne LiDAR scanning in seven periods (2005, 2006, 2009, 2010, 2011, 2012, and 2013) (Imaizumi et al., 2016a). The lowest elevation of each grid cell within the seven periods was assumed to be the bedrock surface elevation. To reduce errors related to the positioning of the aircraft, the DEMs from 2006, 2009, 2010, 2011, 2012, and 2013 were adjusted through comparison with those obtained in 2005 (Imaizumi et al., 2016a). As a result of the adjustment, the mean and standard deviation of the difference in elevation in stable areas between two consecutive DEMs were smaller than 0.1 and 0.3 m, respectively. The depth of channel deposits in the lower Ichinosawa was estimated to be >5 m, as noted above.

**Table 1** Timing of UAV photography and specifications of SfM analyses.

| Date of photography | Average spacing of cloud points (m) | Grid size of DEM (m) | Date of debris flow events | |
|---|---|---|---|---|
| | | | Last event | Next event |
| August 21, 2016 | 0.113 | 0.10 | June 25, 2016 | September 8, 2016 |
| November 20, 2016 | 0.103 | 0.10 | September 20, 2016 | -* |
| May 19, 2017 | 0.055 | 0.10 | -* | June 21, 2017 |
| August 6, 2017 | 0.023 | 0.10 | June 21, 2017 | August 7, 2017 |
| September 15, 2017 | 0.051 | 0.10 | August 7, 2017 | September 17, 2017 |
| September 21, 2017 | 0.068 | 0.10 | September 17, 2017 | October 22, 2017 |
| October 26, 2017 | 0.080 | 0.10 | October 22, 2017 | October 29, 2017 |

| | | | | |
|---|---|---|---|---|
| November 6, 2017 | 0.078 | 0.10 | October 29, 2017 | -* |

* Column is blank because debris flow did not occur before (after) the UAV survey in the year.

# 4. Results

## 4.1. Initiation of debris flow surges

A total of 10 debris flows were observed in 2016 and 2017 (Table 2). The maximum 10-minute rainfall intensity and total rainfall during all debris flow events exceeded 5 and 40 mm, respectively. TLCs were able to capture initiation, runout, and termination processes of debris flow surges during three events (September 8, 2016, June 21, 2017, and October 29, 2017), but the TLCs failed to monitor during the other seven events because of the darkness at night.

**Table 2** List of debris flows in 2016 and 2017.

| Date | Total rainfall (mm) | Maximum 10-min rainfall (mm) | Storage volume before the event ($m^3$) | Total change in the storage volume during the event ($m^3$)*b | TLC monitoring |
|---|---|---|---|---|---|
| May 4, 2016 | 91.0 | 5.3 | – | – | –*a |
| May 11, 2016 | 151.3 | 6.2 | – | – | –*a |
| June 25, 2016 | 49.9 | 10.9 | – | – | –*a |
| September 8, 2016 | 217.1 | 13.2 | >17171 | >2315 | ○ |
| September 20, 2016 | 363.9 | 8.1 | – | – | –*a |
| June 21, 2017 | 180.4 | 6.7 | 29818 | -9 | ○ |
| August 7, 2017 | 203.7 | 8.4 | – | – | –*a |
| September 17, 2017 | 184.9 | 10.1 | 13997 | 2067 | –*a |
| October 22, 2017 | 316.0 | 9.2 | 11930 | 2426 | –*a |
| October 29, 2017 | 192.2 | 10.1 | 9504 | 2119 | ○ |

*a TLCs could not capture debris flow images because of the darkness at night.
*b Difference in storage volume between before and after the debris flow event does not completely agree with total change in the storage volume during the debris flow event, because the area in which topography was successfully measured by UAV-SfM differed among measurement periods.

Multiple surges were monitored by the water pressure sensor during each debris flow event, except the June 21, 2017 event (Fig. 4). On June 21, 2017, TLC monitoring showed that the debris flow, which consisted of only one surge, terminated above the water pressure sensor monitoring site (P19). Therefore, changes in the water level were likely caused by channel bed deformation. Debris flow surges generally began to occur when 10-minute rainfall intensity reached 5 mm. Even when a series of debris flow surges was suspended due to a decrease in rainfall intensity, surges restarted when rainfall intensity reached 5 mm again (e.g., around 15:30 on September 8, 2016; Fig. 4a). Water level was generally lower than 0.05 m in the period without debris flow. However, water level sometimes exceeded 0.1 m in the period without debris flow surges (e.g., 1:30 to 8:30 on September 8, 2016) because of aggradation of the channel bed around the water pressure sensor.

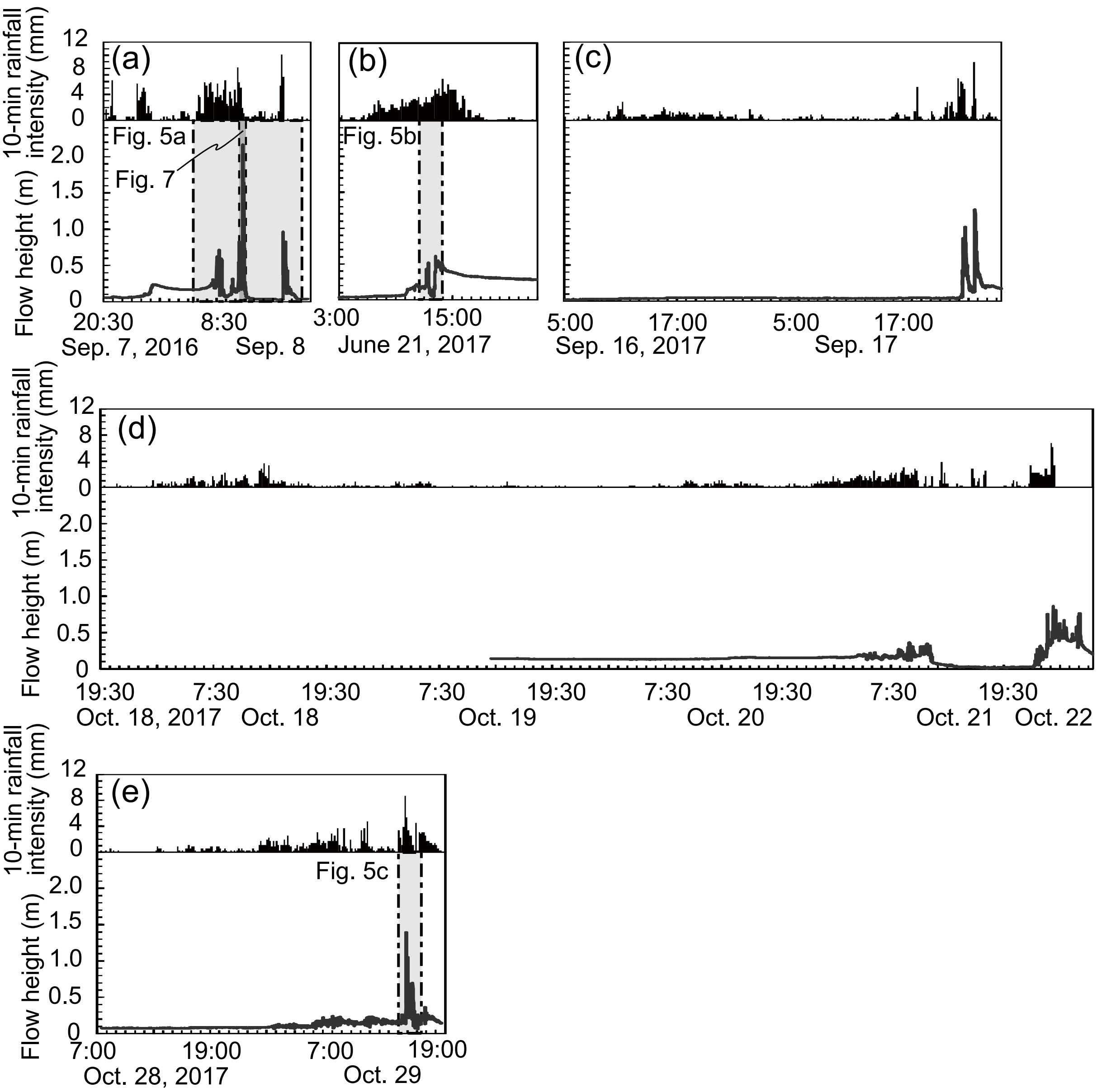


**Figure 4.** Changes in flow height measured by the water pressure sensor at P19 during debris flow events that

were successfully captured by images by TLCs. (a) Debris flow on September 8, 2016. (b) Debris flow on June 21, 2017. (c) Debris flow on September 17, 2017. (d) Debris flow on October 22, 2017. (e) Debris flow on October 29, 2017. Time ranges of Figs. 6 and 8 are shaded gray.

The TLC monitoring revealed that each debris flow surge was formed separately by mobilization of the storage (Fig. 5). Debris flow surges generally started to initiate in upper channel reaches when maximum 10-minute rainfall intensity exceeded 5 mm, and progressively transited downstream after rainfall peaks (Fig. 5a). Three mechanisms of initial movement of soil mass as surges were identified from TLC images, although the mechanism of many surges was not clear because of the long interval between TLC images. One is erosion of channel deposits by overland flow, which mainly occurred in the uppermost section of channel reaches (between P1 and P3). This process was typically identified when overland flow progressed on the unsaturated storage due to increasing water supply from farther upstream. The second mechanism was sliding of channel deposits, for which the travel distance was generally short. The third was sediment supply from the side of the main channel, including the channel bank and tributaries. Bank failures, which occurred due to erosion at the basal part of banks (steepened channel deposits beside the flow path) by stream flow, were mainly monitored in the lower section of upper Ichinosawa (e.g., around P15). Talus slopes at the junction with tributaries also failed due to erosion by stream flow.

When we focused on a specific debris flow event, initiation points of surges were concentrated in specific channel sections. Initiation points of many surges on September 8, 2016 were in sections with deep channel deposits (e.g., >2 m depth) located <30 m below junctions with tributaries and having catchment areas >0.01 $km^2$ (e.g., channel section between P6 and P8; Fig. 6a). Similarly, on June 21, 2017, seventeen surges (61%) initiated in the section between P5 and P6, in which deep channel deposits (>5 m depth) existed near the junction with a large tributary (Fig. 6c). On October 29, 2017, the ratio of surges that initiated within the monitoring section (60%) was lower than that for the other two debris flows (80% and 75% during the September 8, 2016 and June 21, 2017 events, respectively; Figs. 5 and 6). The remaining surges on October 29, 2017 (40%) initiated above P1, where deep storage existed at that time. Thus, the initiation points of surges are likely controlled by the spatial distribution of the storage depth, which varies with time because of the sediment supply from hillslopes and the evacuation of sediment by debris flows (Fig. 6). General characteristics of the initiation points, which are applicable to all three debris flow events, can be expressed by comparison between channel gradient and storage depth (Fig. 7a). Storage depth greater than 2 m is required for the initiation of many surges. In other words, few surges occurred in the monitoring section on October 29, 2017, because storage depth was lower than 2 m in most of the sections. Many surges initiated in the channel section steeper than 25°, but few surges initiated in the section gentler than 20° (Fig. 7a). It was also clear that many debris flows initiated in the section less than 30 m below the junction with tributaries, in which water and sediment are supplied from tributaries.

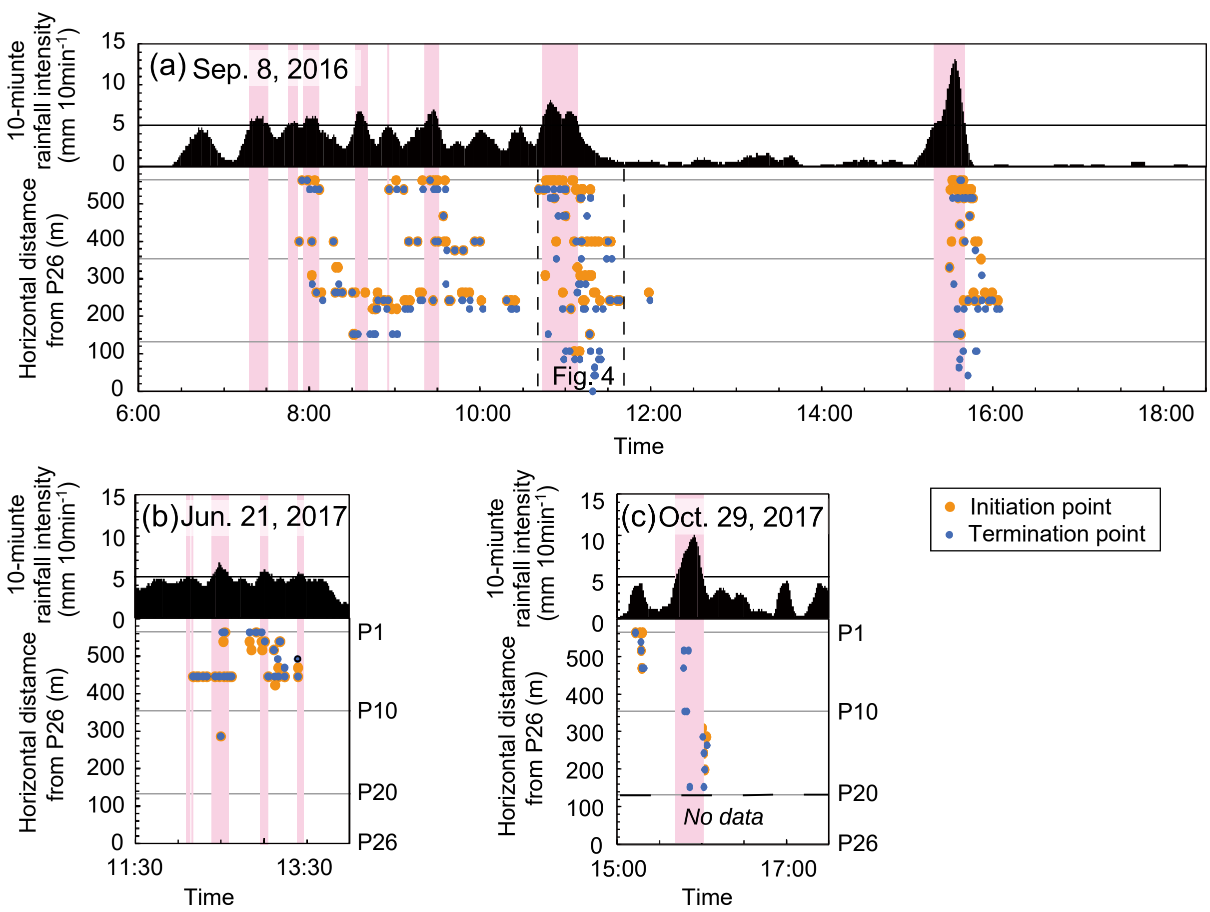


**Figure 5.** Temporal changes in the initiation and termination points of debris flow surges on (a) September 8, 2016, (b) June 21, 2017, and (c) October 29, 2017. Periods with rainfall intensity >5 mm are shaded pink. The

rainfall intensity was calculated from rainfall data with a logging interval of 1 min.

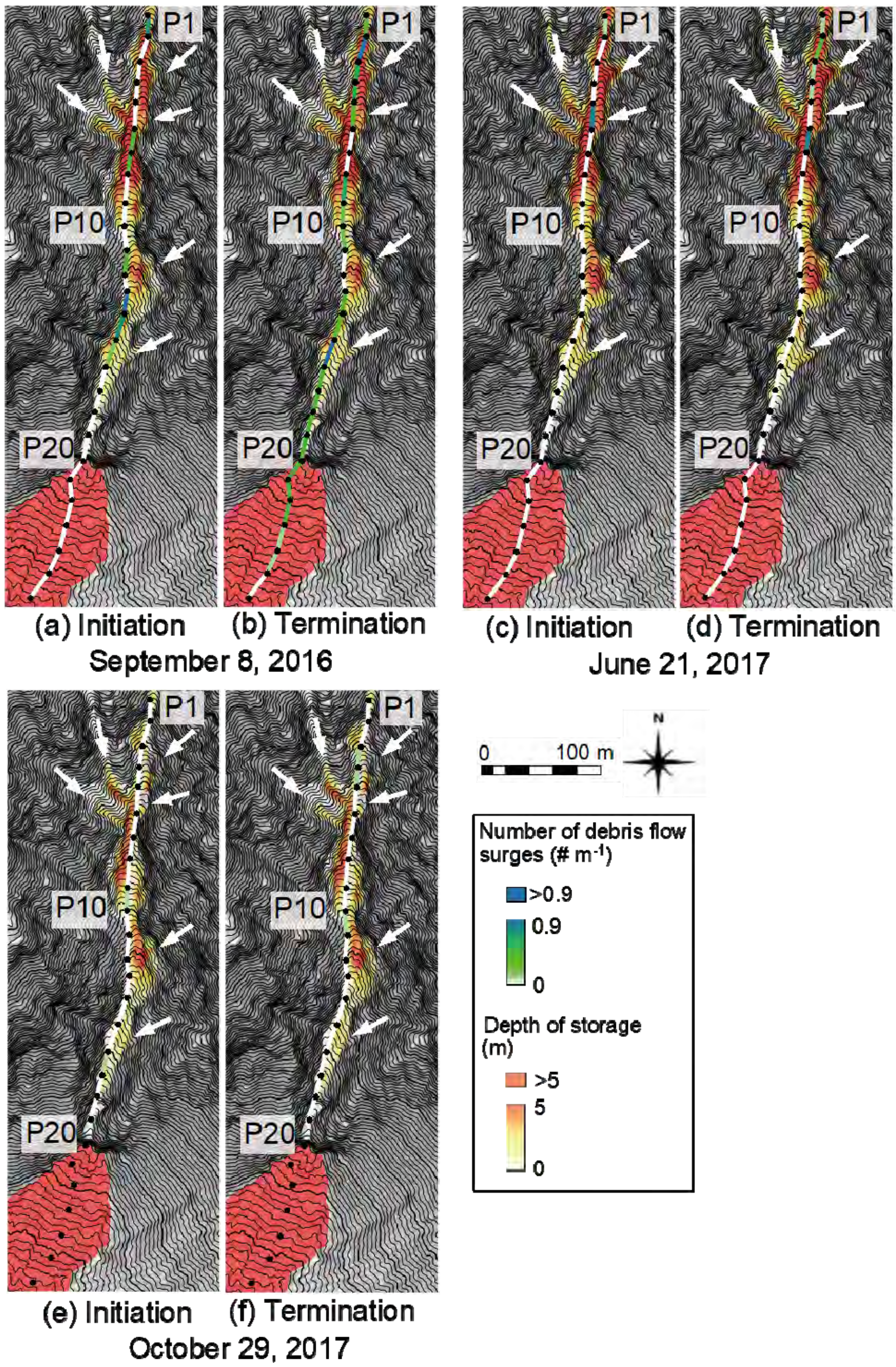


**Figure 6.** Spatial distribution of initiation and termination points of debris flow surges. (a) Initiation points of surges during debris flow on September 8, 2016. (b) Termination points of surges during debris flow on September 8, 2016. (c) Initiation points of surges during debris flow on June 21, 2017. (d) Termination points of surges during debris flow on June 21, 2017. (e) Initiation points of surges during debris flow on September 29, 2017. (f) Termination points of surges during debris flow on September 29, 2017. Locations of junctions with large tributaries are indicated by white arrows.

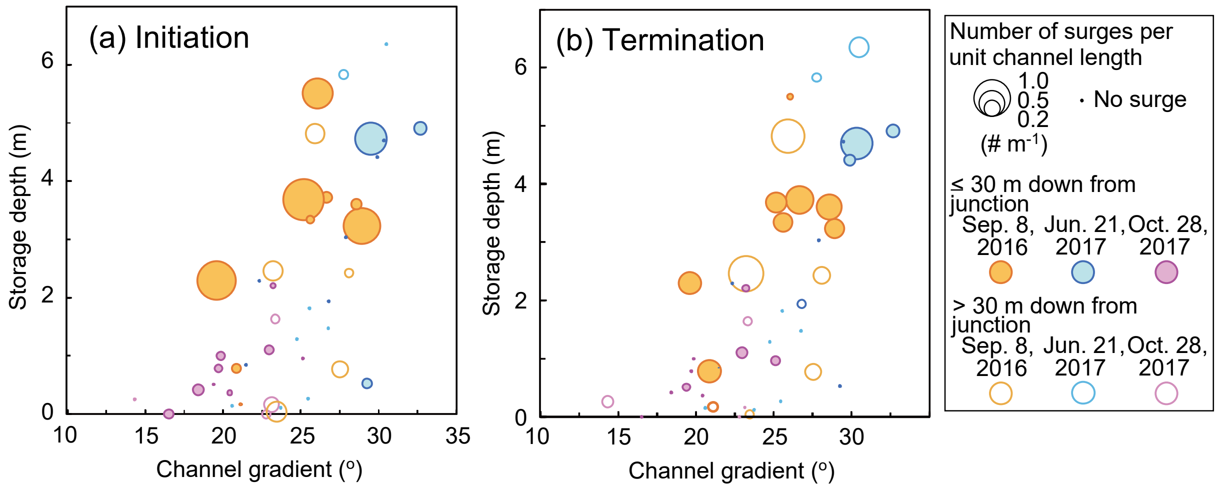


**Figure 7.** Initiation and termination number of surges in each channel section separated by analysis points (P1 to P20) within the upper Ichinosawa. (a) Initiation number of surges in each section. (b) Termination number of surges in each section. Circle sizes indicate the number of surges divided by the length of each channel section (about 20 m). Channel gradient and storage calculated with 1 m intervals along the main channel were averaged in each channel section. The DEM obtained by UAV-SfM just before each debris flow event was used for calculation of the channel gradient and storage depth.

### 4.2. Runout and termination of debris flow surges

As a result of the TLC monitoring, we could successfully observe temporal changes in flow type during a series of surges, as well as the transition of flow type as the surges migrated, which has not previously been reported in detail (Fig. 8). When we focused on a specific channel section, the predominant flow type of each surge changed frequently, even during a single event. Additionally, many surges changed flow type as they flowed downward (Fig. 8).

The duration ratio of each flow type in the entire debris flow was different between the upper and lower parts of the Ichinosawa torrent. On September 8, 2016, the duration of partly saturated flow was clearly longer than that of fully saturated flow in the uppermost reaches of the monitoring section (between P1 and P3), whereas the ratio of fully saturated flow was higher in the lower channel reaches (Fig. 8). On June 21, 2017, surges composed only of partly saturated flow appeared in the upper reaches (above P8), while a surge composed of fully saturated flow was observed in the lower reaches (P13). In this way, the ratio of partly saturated flow was generally higher in the upper channel reaches, while the ratio of fully saturated flow was generally higher in the lower channel reaches. Partly saturated flow preceded the appearance of fully saturated flow during surges composed of both flow types.

The predominant type of flow also differed among the events (Table 3). On June 21, 2017, 96% of all surges whose flow type was identified by TLC images consisted of party saturated flow. In contrast, all surges on October 29, 2017 consisted of fully saturated flow.

Because many surges occurred repetitively and terminated with short travel distance in the upper Ichinosawa, the number of debris flow surges in the upper Ichinosawa (above P20) was clearly higher than that in the lower Ichinosawa (below P20; Fig. 8). The ratio of surges reaching the lower Ichinosawa also differed among debris flow events. On June 21, 2017, all surges terminated within the upper Ichinosawa. In contrast, forty-four percent of surges (11 of 25 surges) reached the debris fan on October 29, 2017. The debris flow surges that reached the lower Ichinosawa usually occurred during rainfall peaks exceeding 5 mm for a long period (e.g., >20 min; Fig. 5). Termination points in the upper Ichinosawa were mainly located in channel sections with deep storage (>2 m), irrespective of the distance from junctions to tributaries (Figs. 6 and 7).

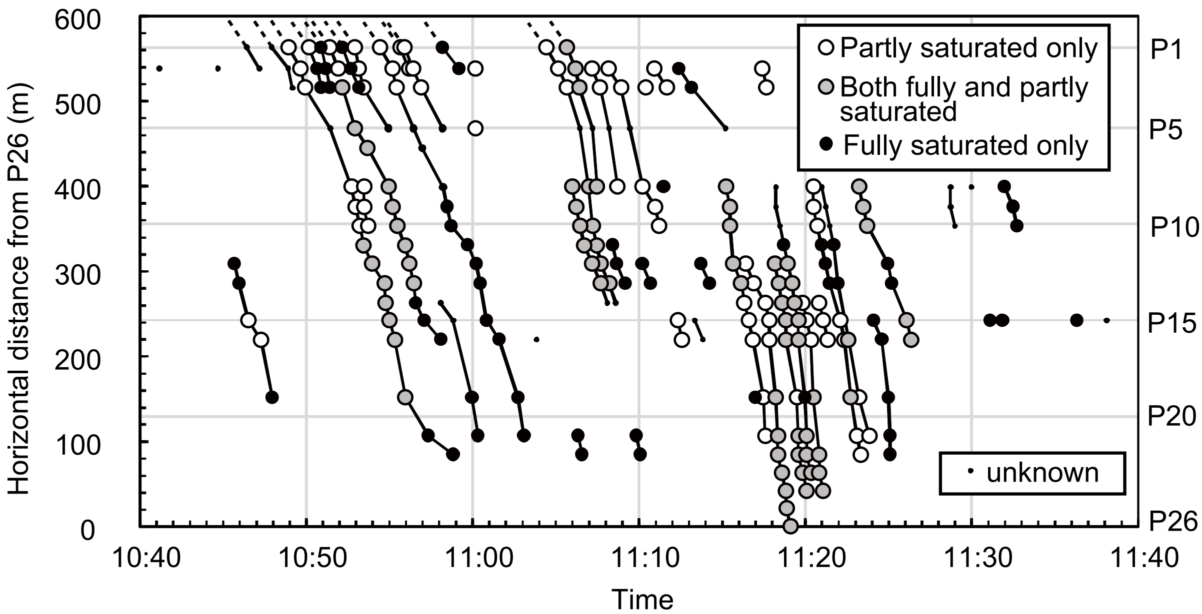


**Figure 8.** Transit time of the head of debris flow surges at each analysis point from 10:40 to 11:40 on September 8, 2016. The flow type obtained from the TLC images was classified into three types: surges

composed only of partly saturated flow from head to tail (Fig. 3a), surges composed of both partly saturated and fully saturated parts (Fig. 3b), and surges composed only of fully saturated flow from head to tail of the surge (Fig. 3c). The flow type was marked "unknown" if the images were not sufficiently clear to determine the flow type. A plot present at the uppermost site (P1) indicates that the surge initiated in the channel section above the monitoring site.

**Table 3** Number of debris flow surges classified into each debris flow types based on analysis of TLC images. "Partly saturated only" indicates that only partly saturated flow was identified from the initiation (appearance) to the termination of surges. The sum of the surge numbers does not correspond to the total number of debris flow surges, because the flow type of some surges was not clear due to fog, the presence of raindrops on the lens of TLCs, or long distance from TLCs to the analysis point. Note that there is a possibility that the TLC monitoring failed to identify the appearance of some flow types because of the long interval between images (15 s).

| | Partly saturated only | Both fully and partly saturated | Fully saturated only |
|---|---|---|---|
| September 8, 2016 | 26 | 35 | 26 |
| June 21, 2017 | 17 | 0 | 1 |
| October 29, 2017 | 0 | 14 | 11 |

## 4.3. Changes in the channel topography caused by debris flows

Changes in the channel bed topography caused by five debris flows, which were successfully measured by UAV-SfM, showed that the locations of erosion and deposition areas differed among debris flow events (Fig. 9). Storage in the upper Ichinosawa (above P20) was significantly eroded by debris flows on September 8, 2016, September 17, 2017, and October 29, 2017 (Figs. 9a, 9c and 9e). Within these three events, the main deposition area of the September 8, 2016 event was located <150 m downward from the Ohya–Ohtaki waterfall (P20), whereas a large part of the sediment entrained by the October 26, 2017 event passed the junction with the Hontani torrent. The channel bed in the upper reaches was aggraded by the debris flow on October 22, 2017. As a result of the UAV survey following the October 22, 2017, event, new deposits derived from some slope failures were identified in the upper part of the basin (Fig. 9d). On June 21, 2017, when no surging was observed at the Ohya waterfall by a TLC, both erosion and deposition areas were located within the upper Ichinosawa, and channel bed deformation was not identified in the lower Ichinosawa (Fig. 9b). The debris flow path changed during the September 8, 2016 and September 17, 2017 events, but the path did not change clearly during the October 22, 2017 and October 29, 2017 events (Fig. 9).

The total volumes of storage evacuated from the upper reaches by debris flows on September 17, October 22, and October 29, 2017 were all within the range of 2000 to 2500 $m^3$ (Table 2). The total change in storage caused by the September 8, 2016 event could not be obtained, because the uppermost part of the valley bottom (< 150 m in length) could not be captured by the UAV. The total volume change by this event was estimated to be less than 3500 $m^3$ based on the loss of storage in the section interpreted by UAV-SfM and the length of channel reaches without topographic data.

Clear erosion of storage with depth >2 m occurred in the channel sections in which many debris flow surges initiated on September 8, 2016 (e.g., channel section between P6 and P8; Figs. 7a and 9a). Clear aggradation was observed in the section where debris flow surges terminated in the lower Ichinosawa (e.g., channel sections P20 to P26 during the September 8, 2016 event; Figs. 6b and 9a), whereas aggradation around termination points in the upper Ichinosawa was not clear (e.g., channel sections P13 and P15 during the September 8, 2016 event; Figs. 5b and 8a). In such sections, TLC monitoring revealed that temporal storage left by previous surges was eroded by subsequent surges that traveled farther downstream.

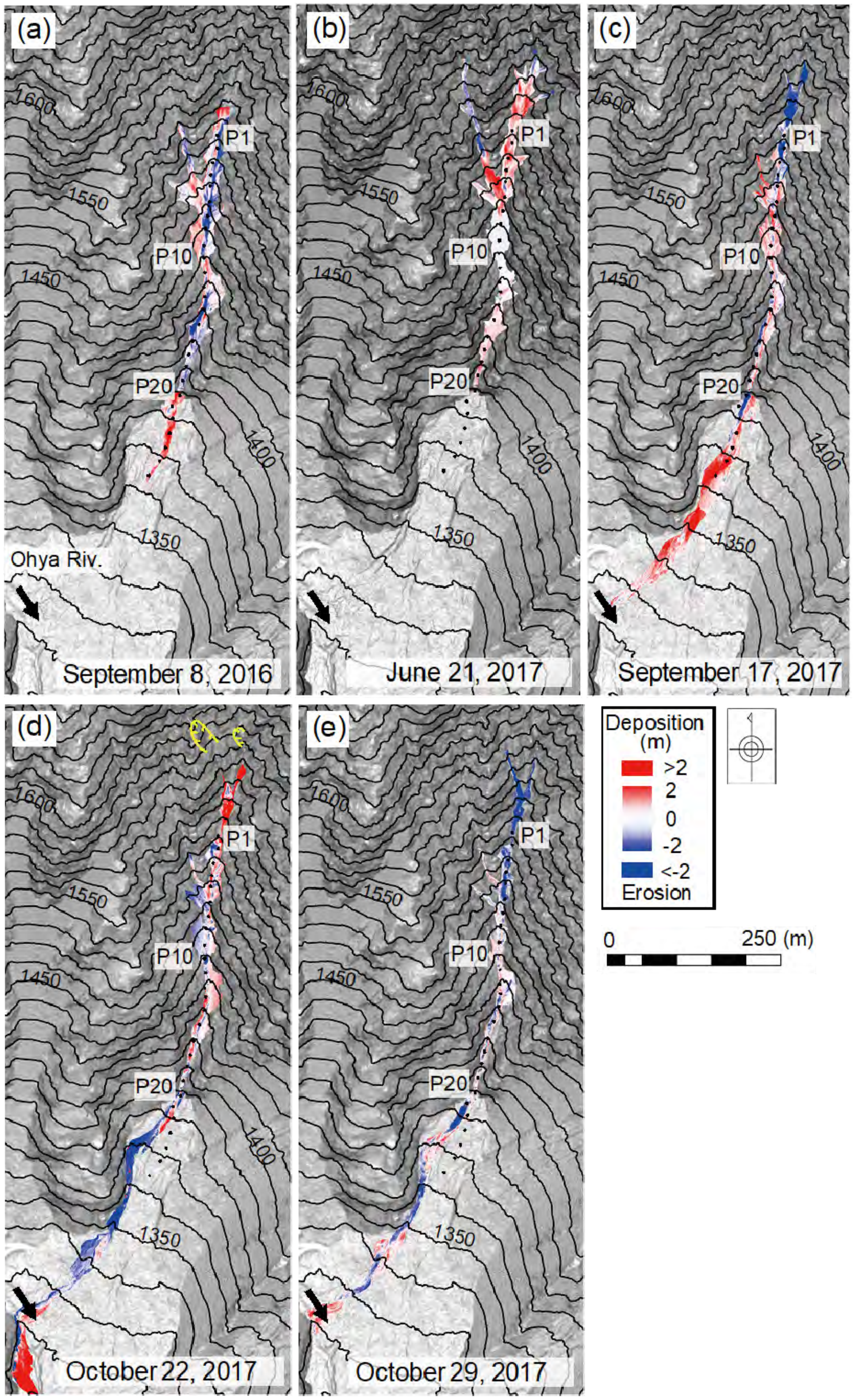


**Figure 9.** Changes in topography caused by debris flows measured by UAV-SfM. (a) Elevation change between August 21, 2016 and November 20, 2016 caused by the debris flow on September 8, 2016. (b) Elevation change between May 19, 2017 and August 6, 2017 caused by the debris flow on June 21, 2017. (c)

Elevation change between September 15, 2017 and September 21, 2017 caused by the debris flow on September 17, 2017. (d) Elevation change between September 21, 2017 and October 26, 2017 caused by the debris flow on October 22, 2017. Locations of slope failure are shown in yellow. (e) Elevation change between October 26, 2017 and November 6, 2017 caused by the debris flow on October 29, 2017. Junction with the Hontani torrent is indicated by the black arrow.

# 5. Discussion

## 5.1. Initiation of debris flow surges

Intensive monitoring using TLCs revealed that debris flow surges initiated separately by erosion of storage by surface flow, sliding of channel deposits, and sediment supply from channel banks and tributaries, rather than through the development of a spontaneous wave on the flow surface because of mechanical instability, which was presented in laboratory experiments and derived by consideration of the flow mechanism (Iverson, 1997; Major, 1997). These three initiation mechanisms monitored by TLCs agree with those reported previously in the Ichinosawa based on video-camera monitoring (Imaizumi et al., 2016b). A large portion of the debris flow surges initiated in channel sections with deep storage (>2 m in depth; Fig. 7), implying that sufficient depth of storage is required for transportation of grouped sediment as a surge. The depth (>2 m) is larger than the size of the largest boulders in the channel, which changes from 1 to 2 m and is associated with the sediment supply from hillslopes and sediment transport by debris flows (Imaizumi et al., 2006, 2016b). Large boulders may resist movement of grouped sediment in cases of shallow storage depth.

Because sediment storage in the upper Ichinosawa has never been completely evacuated by debris flows (Imaizumi et al., 2016a, 2017), the Ichinosawa can be characterized as a transport-limited basin, in which the timing of debris flows is controlled only by that of rainfall exceeding the initiation threshold (Imaizumi et al., 2017). However, fewer debris flow surges occurred in channel sections with thin storage than in sections with thick storage (Fig. 7), indicating that weathering-limited (supply-limited) characteristics, which have been reported in other debris flow torrents (Bovis and Jakob, 1999), occur locally in the Ichinosawa.

Increases in the stream water supplied by tributaries may also be an important factor affecting the formation of surges, because many surges on September 8, 2016 and June 21, 2017 initiated <30 m below the junction with tributaries (Figs. 7 and 8). Previous field monitoring also reported that water supply is one of the most important factors in the initiation of debris flows (Gregoretti et al., 2016; Imaizumi et al., 2016b).

In addition to temporal changes in the initiation point of debris flows among the debris flow events, which have also been reported from other debris flow torrents (Coe et al., 2008; Berger et al., 2011b), temporal changes in the initiation points of surges were monitored even in a single debris flow event (Fig. 5). The initiation point of many surges was located in the upper channel reaches during rainfall peaks, then progressively shifted downstream (Fig. 5). The time lag in runoff peaks between the upper and lower channel reaches was likely affected by the difference in initiation timing of surges among channel sections. In addition, transportation of sediment from the upper to lower reaches by surges around rainfall peaks possibly created the storage accumulation condition that allowed debris flow surges to occur more easily in lower reaches.

Many debris flow surges initiated in channels steeper than 22.2° (Fig. 7), which is the threshold gradient for the occurrence of partly saturated sediment mass (Imaizumi et al., 2017). In addition, partly saturated flow was predominant in the upper part of the monitoring section in the upper Ichinosawa (Fig. 8). Because initiation areas in many other torrents are also steeper than 22.2° (e.g., VanDine, 1985; McCoy et al., 2013), partly saturated debris flows are also considered to be important in other torrents.

## 5.2 Runout and termination of flow

As reported from many other torrents (e.g., Okano et al., 2012; Kean et al., 2013; Hürlimann et al., 2014), the major flow type in the Ichinosawa varied among debris flow events (Table 3). The volume of debris flow material along the channel and the rainfall pattern are considered to be controlling factors affecting the flow type (Okano et al., 2012; Kean et al., 2013; Hürlimann et al., 2014; Staley et al., 2014; Zhou et al., 2015). The debris flow of June 21, 2017, when the volume of storage was the largest of the three events monitored by TLCs, was dominated by partly saturated flow, whereas the debris flow of October 29, 2017, when the volume of storage was the smallest among the three events, was dominated by fully saturated flow (Table 3). This agrees with the previously described trend in the Ichinosawa whereby the ratio of partly saturated flow increases with increases in the volume of storage (Imaizumi et al., 2017). In the Ichinosawa, fully saturated flow is predominant during long-lasting and high total rainfall depth (duration of >5 h, total rainfall depth >50 mm) events, whereas partly saturated flow is predominant during short rainfall events with low total rainfall depth (duration of <5 h, total rainfall depth <50 mm) (Imaizumi et al., 2017). The rainfalls during the three debris flows that could be successfully observed by TLCs in this study were all characterized by long duration and high total rainfall depth. Therefore, the differences in flow type among the three debris flows were likely attributable to the volume of storage within the basin rather than the rainfall pattern.

Channel gradient is considered a factor controlling the solid concentration of a debris flow (Egashira et al., 2001; Takahashi, 2014; Lanzoni et al., 2017). Analysis of the static force at the bottom of flow revealed that partly saturated flow is an important flow type in steeper channel sections (>22.2° in the Ichinosawa), while fully saturated flow is important in gentler channel sections (Imaizumi et al., 2017). Our TLC monitoring showed a trend similar to the trend of those studies: partly and fully saturated flows were predominant in steep channel sections (e.g., above P10 with channel gradient >25°) and gentle channel sections (e.g., below P20 with channel gradient <20°), respectively (Figs. 2 and 8).

Changes in flow type as surges migrated, which has also been monitored in other debris flow torrents (e.g., Hürlimann et al., 2003; Arattano et al., 2012), were frequently monitored in the section between P10 and P15, in which deep channel deposits accumulate (Fig. 8). Some surges lost or shortened their partly saturated part in this section, and only fully saturated flows passed through (Fig. 8). In the Ichinosawa, overland flow is rarely observed in sections with deep sediment storage in the period before the arrival of surges (Imaizumi et al., 2016b), indicating that a large part of the sediment storage is unsaturated, at least in its surficial layer. Decreases in flow mobility, caused by infiltration of interstitial water into unsaturated storage (Staley et al., 2011), likely occurred over such deep storage, resulting in the loss of the partly saturated part of surges. Only fully saturated flow, which contains abundant interstitial water, can pass over such channel sections.

As reported in previous observations in many debris flow torrents (Suwa and Yamakoshi, 1999; Imaizumi et al., 2016a; Wasklewicz and Scheinert, 2016; De Haas et al., 2018), the travel distance of debris flows differed among events (Fig. 8). Most surges during the June 21, 2017 event, which were dominated by partly saturated flow, terminated above P7 (31 of 33 surges; Table 3). In contrast, many surges during the September 8, 2016 and October 29, 2017 events, when many fully saturated flows were observed, flowed down into the lower Ichinosawa (below P20). Because solid concentration is an important factor controlling the mobility of debris flows (Egashira et al., 2001; Takahashi, 2014), high solid concentration and poor interstitial water of the partly saturated flow may have resulted in the shorter travel distance of surges during the June 21, 2017 event than during the other two events.

The travel distance of debris flows also differed among the four debris flows reaching the lower Ichinosawa, although the volume of sediment entrained by these debris flows was not significantly different (Fig. 9, Table 2). Many debris flow surges terminated in the upper part of the debris flow fan (just below P20) on September 8, 2016 (Fig. 7b). Decreases in the channel gradient at P20 (Fig. 2), which in turn decrease the upper limit of solid concentration in debris flow (Egashira et al., 2001; Takahashi, 2014; Lanzoni et al., 2017), likely facilitated the termination of the surges. In contrast, debris flows on September 17, 2017, October 22, 2017, and October 29, 2017 flowed farther downstream. Because total rainfall depth and maximum 10-minute rainfall intensity on September 17, 2017 and October 29, 2017 were lower than those on September 8, 2016 (Table 2), the difference in rainfall amount was not an important factor controlling the travel distance of these debris flow events. The solid concentration in surges during the September 8, 2016 event was possibly higher than in other debris flows because of the large volume of storage (Table 2), resulting in the short travel distance.

Additionally, the travel distance was different among surges even in a single debris flow event comprising multiple surges (Figs. 5 and 8). Rainfall pattern, rather than volume of storage, affected the travel distance of individual surges. When the rainfall intensity exceeded 5 mm 10 min$^{-1}$ for a long period (e.g., around 11:00 and 15:30 on September 8, 2016 and 15:50 on October 29, 2017), many surges reached below P20 (Fig. 5). Abundant water supply from continuous intensive rainfall likely increases the mobility of surges.

## 5.3 Channel bed changes caused by each surge and the entire debris flow

On September 8, 2016, although only significant erosion was identified by the UAV-SfM monitoring in the upper Ichinosawa (Fig. 9a), TLC images revealed frequent degradation and aggradation according to the initiation and termination of surges during the debris flow event. This indicates that temporal changes in channel topography are not as simple as those estimated from net changes in topography over an entire event. On September 8, 2016 and October 29, 2017, TLCs captured some debris flow surges initiating on channel deposits that were left by previous debris flow surges. Therefore, changes in the spatial distribution of storage by previous surges also affects the initiation point of subsequent surges.

Avulsion of the debris flow path, which is a common phenomenon on debris flow fans worldwide (e.g., Suwa and Okuda, 1983; Imaizumi et al., 2016a, de Hass et al., 2018), was monitored during the September 8, 2016 and September 17, 2017 events (Fig. 9). De Hass et al. (2018) reported that avulsion of the debris flow path occurs by the formation of plugs when mobility of the debris flow is low. During the event of September 8, 2016, some surges on the debris flow fan were composed of partly saturated flow (Fig. 8), which generally has low flow mobility (Imaizumi et al., 2006; Imaizumi et al., 2017). Although the debris flow on September 17, 2017 could not be monitored by TLCs, it is likely that partly saturated flows were dominant because of the large volume of storage before the event (Table 3). Therefore, low mobility of the debris flow surges, particularly those formed by partly saturated flow, possibly affected avulsion of the debris flow path during the two events. In contrast, the mobility of the surges on October 22 and October 29, 2017, which did not cause avulsion of the debris flow path (Fig. 9), is considered to be high because of the small volume of storage before the event.

## 6. Summary and Conclusion

To clarify the initiation and runout characteristics of debris flow surges, we conducted field monitoring in the Ohya landslide scar, where debris flows occur frequently according to the mobilization of storage (e.g., channel deposits and talus slopes). Using TLCs, we successfully obtained data on initiation, runout, and termination processes of surges that occurred repetitively during each debris flow event. Debris flow surges were mainly formed by repetitive mass movement of storage within a debris flow initiation zone. The development of spontaneous waves on the flow surface was not an important formation process of the surges.

Because many surges occurred in channel sections with deep storage (>2 m in depth) near junctions with large tributaries, the existence of debris flow material and water supply are likely important for the formation of surges. Partly saturated flow is the predominant flow type in the steep initiation zones, and fully saturated flow is the predominant flow type in gentle transportation and deposition zones. The volume of storage in the initiation zone likely affected flow type, travel distance of surges, and avulsion of flow path on a debris flow fan by controlling the mobility of surges.

Our study elucidated that characteristics of surges, such as flow type, travel distance, and locations of erosion and deposition, differ not only among debris flow events, but also among surges within a single debris flow event. The significant erosion and deposition of sediment by a debris flow, identified by comparison of topography before versus after an event, result from repetitive erosion and deposition by individual surges with various characteristics. Therefore, periodic measurement of the topography is insufficient when attempting to understand the behavior of surges. Our monitoring also showed that monitoring systems in lower channel reaches cannot observe all debris flow surges that form in initiation zones, because many surges terminate in the upper part of the torrent. Additionally, the flow type of surges in the initiation zone of debris flows is different from that in lower reaches because of differences in channel gradient. Consequently, monitoring of debris flows at multiple points is required to understand the series of processes from initiation to termination.

**Acknowledgement**

This study was supported by JSPS Grant Numbers 18H02235, 18K18917, and 17H02029. Airborne DEM was provided by Shizuoka River Office, Chubu Regional Bureau, Ministry of Land, Infrastructure, Transport and Tourism, Japan.

## References

Abancó, C., Hürlimann, M., Moya J., 2014. Analysis of the ground vibration generated by debris flows and other torrential processes at the Rebaixader monitoring site (Central Pyrenees, Spain). Nat. Hazards Earth

Syst. Sci., 14, 929–943. https://doi.org/10.5194/nhess-14-929-2014

Arattano, M., 1999. On the use of seismic detectors as monitoring and warning system for debris flows. Nat. Hazards, 20, 197–213. https://doi.org/10.1023/A:1008061916445

Arattano, M., Marchi, L., Cavalli, M., 2012. Analysis of debris-flow recordings in an instrumented basin: confirmations and new findings. Nat. Hazards Earth Syst. Sci. 12, 679–686. https://doi.org/10.5194/nhess-12-679-2012

Berger, C., McArdell, B.W., Schlunegger, F., 2011a. Sediment transfer patterns at the Illgraben catchment, Switzerland: Implications for the time scales of debris flow activities. Geomorphology 125, 421–432. https://doi.org/10.1016/j.geomorph.2010.10.019

Berger, C., McArdell, B.W., Schlunegger, F., 2011b. Direct measurement of channel erosion by debris flows, Illgraben, Switzerland. *J. Geophy. Res.* Earth Surface 116, F01002. https://doi.org/10.1029/2010JF001722

Berti, M., Genevois, R., Simoni, A., Tecca, P.R., 1999. Field observations of a debris flow event in the Dolomites. Geomorphology 29, 265–274. https://doi.org/10.1016/S0169-555X(99)00018-5

Bovis, M. J., Jakob, M., 1999. The roll of debris supply conditions in predicting debris flow activity. Earth Surf. Process. Landf. 24, 1039–1054. https://doi.org/10.1002/(SICI)1096-9837(199910)24:11<1039::AID-ESP29>3.0.CO;2-U

Chen C.Y., Chen, T.C., Yu, F.C., Hung, F.Y., 2004. A landslide dam breach induced debris flow – a case study on downstream hazard areas delineation. Environ. Geol. 47, 91–101, https://doi.org/10.1007/s00254-004-1137-6

Chen, H.X., Zhang, L.M., Chang, D.S., Zhang, S., 2012. Mechanisms and runout characteristics of the rainfall triggered debris flow in Xiaojiagou in Sichuan Province, China. Nat. Hazards 62, 1037–1057. https://doi.org/10.1007/s11069-012-0133-5

Chen, H.Y., Cui, P., Zhou, G.G.D., Zhu, X.H., Tang J.B., 2014. Experimental study of debris flow caused by domino failures of landslide dams. Int. J. Sediment Res. 29, 414-422. https://doi.org/10.1016/S1001-6279(14)60055-X

Coe, J.A., Kinner, D.A., Godt, J.W., 2008. Initiation conditions for debris flows generated by runoff at Chalk

Cliffs, central Colorado. Geomorphology 96, 270–297. https://doi.org/10.1016/j.geomorph.2007.03.017

Coussot, P., Meunie, M., 1996. Recognition, classification and mechanical description of debris flows. Earth-Sci. Rev. 40, 209–227. https://doi.org/10.1016/0012-8252(95)00065-8

Degetto, M., Gregoretti, C., Bernard, M., 2015. Comparative analysis of the differences between using LiDAR contourbased DEMs for hydrological modeling of runoff generating debris flows in the Dolomites. Front. Earth Sci. 3, 21. https://doi.org/10.3389/feart.2015.00021.

De Haas, T., Densmore, A.L., Stoffel, M., Suwa, H., Imaizumi, F., Ballesteros-Cánovas, J.A., Wasklewicz, T., 2018. Avulsions and the spatio-temporal evolution of debris-flow fans. Earth-Sci. Rev. 117, 53–75. https://doi.org/10.1016/j.earscirev.2017.11.007

Egashira, S., Itoh, T., Takeuchi, H., 2001. Transition mechanism of debris flows over rigid bed to over erodible bed. Phys. Chem. Earth, Part, Part B: Hydrology, Oceans and Atmosphere 26, 169–174. https://doi.org/10.1016/S1464-1909(00)00235-5

Gregoretti, C., Dalla Fontana, D., 2008. The triggering of debris flow due to channel-bed failure in some alpine headwater basins of the Dolomites: analyses of critical runoff. Hydrol. Process. 22, 2248–2263. https://doi.org/10.1002/hyp.6821

Gregoretti, C., Degetto, M., Bernard, M., Crucil, G., Pimazzoni, A., De Vido, G., Berti, M., Simoni, A., Lanzoni, S., 2016. Runoff of small rocky headwater catchments: Field observations and hydrological modeling. Water Resour. Res. 52, 8138–8158. https://doi.org/10.1002/2016WR018675

Hürlimann, M., Abancó, C., Moya, J., Vilajosana, I., 2014. Results and experiences gathered at the Rebaixader debris-flow monitoring site, Central Pyrenees, Spain. Landslides 11, 939–953, https://doi.org/10.1007/s10346-013-0452-y

Hürlimann, M., Rickenmann, D., Graf, C., 2003. Field and monitoring data of debris-flow events in the Swiss Alps. Can. Geotech. J. 40, 161–175. https://doi.org/10.1139/t02-087

Imaizumi, F., Hayakawa, Y.S., Hotta, N., Tsunetaka, H., Ohsaka, O., Tsuchiya, S., 2017. Relationship between the accumulation of sediment storage and debris-flow characteristics in a debris-flow initiation zone, Ohya landslide body, Japan. Nat. Hazards Earth Syst. Sci. 17, 1923–1938.

https://doi.org/10.5194/nhess-17-1923-2017

Imaizumi, F., Tsuchiya, S., Ohsaka, O., 2005. Behaviour of debris flows located in a mountainous torrent on the Ohya landslide, Japan. Can. Geotech. J. 42, 919–931. https://doi.org/10.1139/t05-019

Imaizumi, F., Sidle, R. C., Tsuchiya, S., Ohsaka, O., 2006. Hydrogeomorphic processes in a steep debris flow initiation zone. Geophys. Res. Lett. 33, L10404. https://doi.org/10.1029/2006GL026250

Imaizumi, F., Sidle, R.C., Kamei, R., 2008. Effects of forest harvesting on the occurrence of landslides and debris flows in steep terrain of central Japan. Earth Surf. Process. Landf. 33, 827–840. https://doi.org/10.1002/esp.1574

Imaizumi, F., Trappman, D., Matsuoka, N., Tsuchiya, S., Ohsaka, O., Stoffel, M., 2016a. Biographical sketch of a giant: deciphering recent debris-flow dynamics from Ohya landslide body (Japanese Alps). Geomorphology 272, 102–114. https://doi.org/10.1016/j.geomorph.2015.11.008

Imaizumi F., Tsuchiya, S., Ohsaka, O., 2016b. Field observations of debris-flow initiation processes on sediment deposits in a previous deep-seated landslide site. J. Mount. Sci. 13, 213–222. https://doi.org/10.1007/s11629-015-3345-9

Iverson, R. M., 1997. The physics of debris flows. Rev. Geophys. 35, 245–296.

Iverson, R.M., George, D.L., 2016. Modelling landslide liquefaction, mobility bifurcation and the dynamics of the 2014 Oso disaster, Géotechnique 66, 175–187. https://doi.org/10.1680/jgeot.15.LM.004

Iverson, R.M., Ouyang, C., 2015. Entrainment of bed material by Earth-surface mass flows: Review and reformulation of depth-integrated theory, Rev. Geophys., 53, 27–58. https://doi.org/10.1002/2013RG000447

Jakob, M., Bovis, M., Oden, M., 2005. The significance of channel recharge rates for estimating debris-flow magnitude and frequency. Earth Surf. Process. Landf. 30, 755–766. https://doi.org/10.1002/esp.1188

Kean, J.W., McCoy, S.W., Tucker, G.E., Staley, D.M., Coe, J.A., 2013. Runoff-generated debris flows: Observations and modeling of surge initiation, magnitude, and frequency. J. Geophys. Res. Earth Surface 18, 2190–2207. https://doi.org/10.1002/jgrf.20148

Lanzoni, S. Gregoretti, C., Stancanelli, L.M., 2017. Coarse-grained debris flow dynamics on erodible beds. J.

Geophys. Res. Earth Surface 122, 592–614. https://doi.org/10.1002/2016JF004046

Major, J., 1997. Depositional processes in large-scale debris-flow experiments. J. Geol. 105, 345-366. https://doi.org/10.1086/515930

McCoy, S.W., Tucker, G.E., Kean, J.W., Coe, J.A., 2013. Field measurement of basal forces generated by erosive debris flows. J. Geophys. Res. Earth Surface 118, 589–602. https://doi.org/10.1002/jgrf.20041

Neugirg, F., Stark, M., Kaiser, A., Vlacilova, M., Della Seta, M., Vergari, F., Schmidt, J., Becht, M., Haas, F., 2016. Erosion processes in calanchi in the Upper Orcia Valley, Southern Tuscany, Italy based on multitemporal high-resolution terrestrial LiDAR and UAV surveys. Geomorphology 269, 8–22. https://doi.org/10.1016/j.geomorph.2016.06.027

Ogiso, M., Yomogida, K., 2015. Estimation of locations and migration of debris flows on Izu-Oshima Island, Japan, on 16 October 2013 by the distribution of high frequency seismic amplitudes. J. Volcanol. Geotherm. Res. 298, 15–26. https://doi.org/10.1016/j.jvolgeores.2015.03.015

Okano, K., Suwa, H., Kanno, T., 2012. Characterization of debris flows by rainstorm condition at a torrent on the Mount Yakedake volcano, Japan. Geomorphology 136, 88–94. https://doi.org/10.1016/j.geomorph.2011.04.006

Schlunegger, F., Badoux, A., McArdell, B.W., Gwerder, C., Schnydrig, D., Rieke-Zapp, D., Molnar, P., 2009. Limits of sediment transfer in an alpine debris-flow catchment, Illgraben, Switzerland. Quat. Sci. Rev. 28, 1097–1105. https://doi.org/10.1016/j.quascirev.2008.10.025

Schraml, K., Oismüller, M., Stoffel, M., Hübl, J., Kaitna, R., 2015. Debris-flow activity in five adjacent gullies in a limestone mountain range. Geochronometria 42, 60–66. https://doi.org/10.1515/geochr-2015-0007

Staley, D.M., Wasklewicz, T.A., Coe, J.A., Kean, J.W., McCoy, S.W., Tucker, G.E., 2011. Observations of debris flows at Chalk Cliffs, Colorado, USA: Part 2, changes in surface morphometry from terrestrial laser scanning in the summer of 2009. Ital. J. Eng. Geol. Env. – Book, 5th International Conference on Debris-Flow Hazards Mitigation: Mechanics, Prediction and Assessment, 759–768. https://doi.org/10.4408/IJEGE.2011-03.B-083

Staley, D.N., Wasklewicz, T.A., Kean, J.W., 2014. Characterizing the primary material sources and dominant erosional processes for post-fire debris-flow initiation in a headwater basin using multi-temporal terrestrial laser scanning data. Geomorphology 214, 324–338. https://doi.org/10.1016/j.geomorph.2014.02.015

Suwa, H., Okuda, S., 1983. Deposition of debris flows on a fan surface, Mt. Yakedake, Japan. Zeitschrift fur Geomorphologie NF Supplementband 46, 79–101.

Suwa, H., Yamakoshi, T., 1999. Sediment discharge by storm runoff at volcanic torrents affected by eruption. Zeitschrift fur Geomorphologie NF Supplementband 114, 63–88.

Takahashi, T., 1991. Debris flow, IAHR Monograph. A.A. Balkema, Rotterdam.

Takahashi, T., 2014. Debris flow, CRC Press/Balkema, EH Leiden, the Netherlands.

Theule, J.I., Li´ebault, F., Loye, A., Laigle, D., Jaboyedoff, M., 2012. Sediment budget monitoring of debris-flow and bedload transport in the Manival Torrent, SE France. Nat. Hazards Earth Syst. Sci. 12, 731–749. https://doi.org/10.5194/nhess-12-731-2012

Tsuchiya, S., Imaizumi, F., 2010. Large sediment movement caused by the catastrophic Ohya-kuzure landslide. J. Dis. Sci. 3(5), 257–263.

VanDine, D.F., 1985. Debris flows and debris torrents in the southern Canadian Cordillera. Can. Geotech. J. 22, 44–62. https://doi.org/10.1139/t85-006

Wasklewicz, T., Scheinert, C., 2016. Development and maintenance of a telescoping debris flow fan in response to human-induced fan surface channelization, Chalk Creek Valley natural debris flow laboratory, Colorado, USA. Geomorphology 252, 51–65. https://doi.org/10.1016/j.geomorph.2015.06.033

Zhou, G.G.D., Cui, P., Tang, J.B., Chen, H.Y., Zou, Q., Sun, Q.C., 2015. Experimental study on the triggering mechanisms and kinematic properties of large debris flows in Wenjia Gully. Eng. Geol. 194, 52–61. https://doi.org/10.1016/j.enggeo.2014.10.021